FINITE ELEMENT ANALYSIS OF STEEL BEAM-CFST COLUMN JOINTS WITH BLIND BOLTS

Md. Kamrul Hassan[1], Zhong Tao[2], Olivia Mirza[3], Tian-Yi Song[4], Lin-Hai Han[5]

ABSTRACT: *The combined utilisation of concrete-filled steel tubular (CFST) columns and steel beams has increased in composite building construction in recent years. The steel tube of a CFST column normally provides the confinement to the concrete, whilst the concrete restrains the local buckling of the steel tube. The connections between the steel beams and CFST columns can be designed as rigid connection, pinned connection or semi-rigid connection. Known as semi-rigid connections, the endplate connections are gaining popularity due to the ease of installation. This paper investigates the steel beam-CFST column joints with endplate connections, in which the blind bolts are used. The behaviour of the connections is investigated using finite element (FE) analysis. The FE simulation results are compared with test data to verify the FE model. The influence of different types of blind bolts and binding bars on the joint behaviour is analysed.*

KEYWORDS: FE modelling, Blind bolt, Endplate connection, CFST column

1 INTRODUCTION

The use of concrete-filled steel tubular (CFST) columns has increased in recent years due to many structural and construction benefits [1-2]. The steel tube of a CFST column normally provides confinement to the concrete, while the concrete restrains the local buckling of the steel tube. And hence the combined utilisation of CFST columns and steel beams has become an attractive option in the composite building construction for low-rise and high-rise buildings [3]. However, the connections between steel beams and CFST columns are more complicated compared to those in a steel structure. In steel structures, only the homogeneous steel material is used for the construction of columns and beams, but dissimilar materials such as steel in thin-walled tubes and concrete are used for fabricating CFST columns. These types of connections can be designed either as rigid, pinned or semi-rigid connections. In a rigid connection, the steel beam is welded to the thin-walled steel tube of the CFST column; and in a pinned connection, fin plate connections are often used where the fin plates are welded to the steel tube of the CFST column and bolted with the beam web. In the construction of semi-rigid connections, endplate connections are gaining popularity [3-4] due to the ease of installation in which endplates are welded to steel beams and bolted with the steel tube of the CFST column using blind bolts. The blind-bolted system overcomes the lack of access inside the steel tube of the CFST column. These types of bolts can be installed from the outer side of the steel tube and there is no need to access inside the steel tube during tightening or installation of the bolts.

Experimental studies on blind-bolted endplate connections have been conducted in the past to investigate the behaviour of connections. As experimental investigations are expensive and time consuming, the development of finite element (FE) models, well validated against experimental data, would form a useful alternative to overcome any experimental limitations. FE analysis can be a reliable method for investigating the effect of all relevant parameters of the steel beam to CFST column connections [5]. However, the modelling of the blind-bolted end plate connection to connect the steel beam to CFST column is normally different from the modelling of a normal bolted endplate connection to connect the steel beam to steel column. The main differences between these two models are in bolt geometry, contact of the bolt portion with concrete, and contact between the concrete core and steel tube of the CFST column.

In this paper, the modelling details of blind-bolted endplate connections to connect steel beams and CFST columns are illustrated and the FE model is validated with experimental test data. A parametric analysis is also conducted to check the influence of different types of blind bolts, as well as the existence of binding bars. The binding bars are used

[1] Md. Kamrul Hassan, Institute for Infrastructure Engineering, University of Western Sydney. Email: k.hassan@uws.edu.au
[2] Zhong Tao, Institute for Infrastructure Engineering, University of Western Sydney. Email: z.tao@uws.edu.au
[3] Olivia Mirza, School of Computing, Engineering and Mathematics, University of Western Sydney. Email: o.mirza@uws.edu.au
[4] Tian-Yi Song, Institute for Infrastructure Engineering, University of Western Sydney. Email: t.song@uws.edu.au
[5] Lin-Hai Han, Department of Civil Engineering, Tsinghua University. Email: lhhan@tsinghua.edu.au

as stiffeners for the steel tube to enhance the composite action between the steel tube and concrete core of the CFST column.

2 FINITE ELEMENT MODEL

The FE modelling using ABAQUS software depends on the proper consideration of the element type, contact interaction, material modelling and analysis system, which are illustrated in the following sub-sections.

2.1 SELECTION OF ELEMENTS

The most common types of elements available in ABAQUS library include shell elements (S4R), three dimensional solid elements (C3D8, C3D8H, C3D8I, C3D8R, C3D20, C3D20H, C3D20R), truss elements (T3D2), and connector elements. Shell elements (S4R) can be used to model the steel tube and steel beam. In this paper, solid elements are used to model components such as the steel tube, concrete, endplate, bolts, shear connectors and binding bars. Different continuum or solid elements are considered including eight-node linear (first-order) elements (C3D8, C3D8H, C3D8I, C3D8R) and twenty-node quadratic (second-order) elements (C3D20, C3D20H, C3D20R). Each element type has some advantages and disadvantages. Care should be taken in choosing suitable elements for the steel tube connected with a steel beam when the beam is subjected to tension or high bending moment.

An element sensitivity analysis for a steel beam-square hollow section (SHS) column joint is conducted in which the axial load is applied along the axial direction of the steel beam (Figure 1). Figure 2 shows the element sensitivity analysis results for different mesh sizes (MS) (30 mm, 25 mm, 20 mm, 15 mm and 10 mm) with different types of elements. It is observed that if C3D8 and C3D8R elements are used in the modelling, the model result, in terms of load-displacement curve, varies with the mesh size (as shown in Figure 2 (a)-(b)). The coarse mesh (30 mm) model shows higher stiffness,

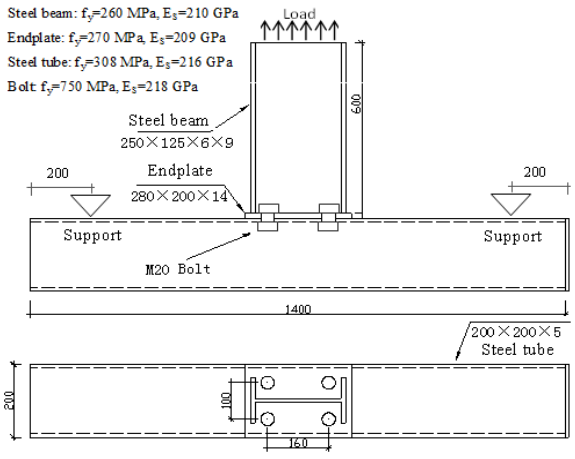

Figure 1: *Configuration details of a steel beam-SHS column joint*

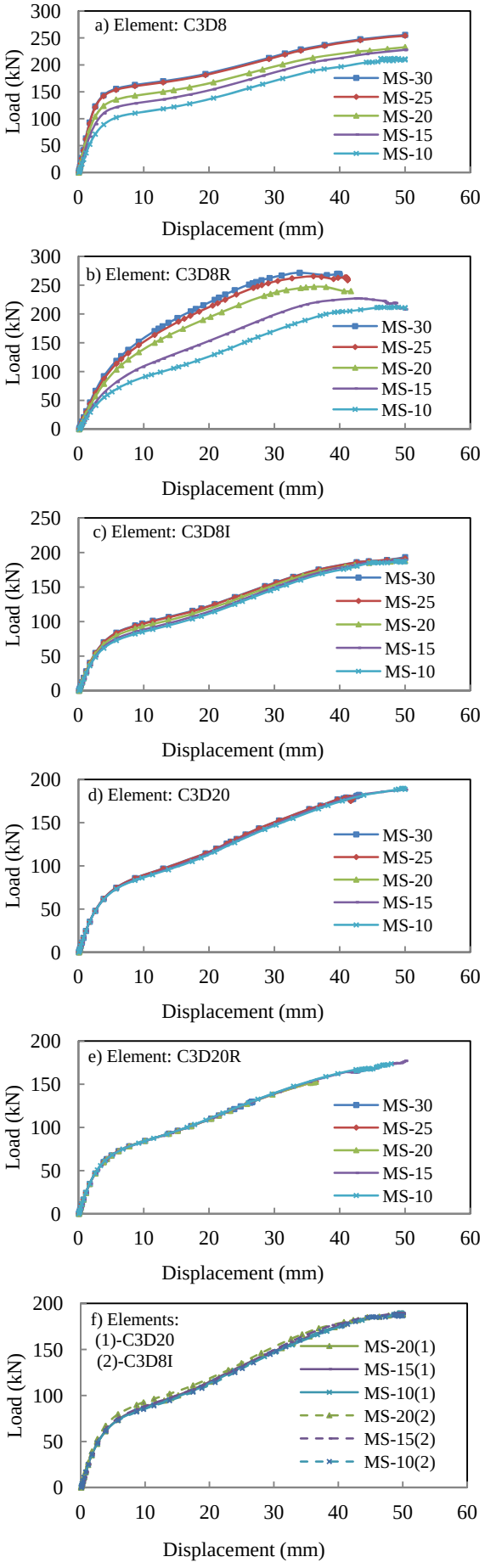

Figure 2: *Element sensitivity analysis for a steel beam-SHS column joint*

but finer mesh (10 mm) model shows lower stiffness. On the other hand, other elements (C3D8I, C3D20 and C3D20R as shown in Figure 1(c)-(f)) give converged results in both coarse mesh and fine mesh cases. For C3D20 and C3D20R elements, the accuracy of the results is higher. However, the computation time for this element (C3D20 and C3D20R) is also higher compared to that when the C3D8I element is used. It is also seen that for C3D8I elements, there is no significant difference with C3D20 and C3D20R elements for both coarse mesh and fine mesh in terms of prediction results. This is because the C3D8I element is an improved version of the C3D8 element. It is introduced to remove the shear locking and reduce the volumetric locking. The internal deformation modes are added to the standard displacement modes of the element in order to eliminate the parasitic shear stresses that occur in bending. So incompatible mode elements (C3D8I) are used hereafter to model components such as the steel tube, endplate, bolt, concrete core, and steel beam. The C3D8I elements are also recommended by other researchers [5-6] for bending and contact problems.

2.2 BLIND BOLTS MODELLING

Bolt that can be tightened from one side is known as blind bolt. There are four types of blind bolts including the Flowdrill system, the Huck Blind bolt, the Ajax Oneside bolt, and the Lindapter Hollo-bolt. Lindapter Hollo-bolt is also known as Hollo-bolt. The geometry of the Hollo-bolt, after tightening, is different from other blind bolts. The main difference is on the inner part of the bolt especially the bolt nut area. When Hollo-bolts are tightened using a torque wrench, the thread truncated cone is draw into the sleeve, spreading the legs of the sleeve and forming a secure clamping against pull out. In addition, the bolt nut for the Hollo-bolt is in a cone shape, but for standard bolts, it is a hexagonal shape. The Hollo-bolt clamping area is different from that of other blind bolts. Other blind bolt clamping areas are similar to that of a standard bolt due to the similar nut shape after bolt tightening. In FE analysis, the modelling of Hollo-bolt is therefore not similar to that of standard bolts due to the different nut shape and clamping condition. For the FE modelling, a simplified Hollo-bolt model is introduced as shown in Figure 3. The Hollo-bolt has five components including the bolt head, collar, sleeve, solid cone and bolt shank, and all of these components are considered as one solid part. Hexagonal bolt heads and collars of blind bolts are idealised as circular bolt heads and collars to simplify the analysis. The reason for the consideration of one solid part of the whole Hollo-bolt is to avoid the convergence problem. The angle of the solid cone of the modified blind bolt is considered the same as the cone slope of the original blind bolt. FE models of endplate connections with blind bolts and standard bolts are shown in Figure 4. The dimension details of simplified blind bolts of M16 and M20 of grade 8.8 are given in Table 1.

2.3 CONTACT MODELLING

To define the contact interaction in the FE modelling, there are three different types of contact options available in ABAQUS/Standard: general contact, surface-to-surface contact and self-contact. In blind-bolted endplate connection modelling, surface-to-surface contact is used to simulate the contact interaction between components and to transfer compressive load from one component to

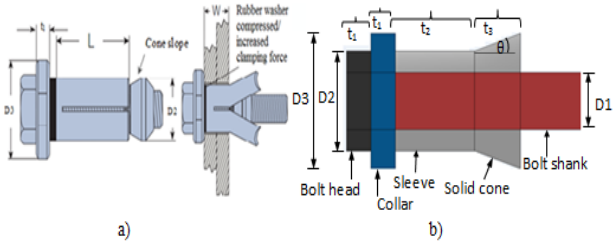

Figure 3: *Geometry details of the blind bolt: a) Original blind bolt (Hollo-bolt), b) Simplified blind bolt*

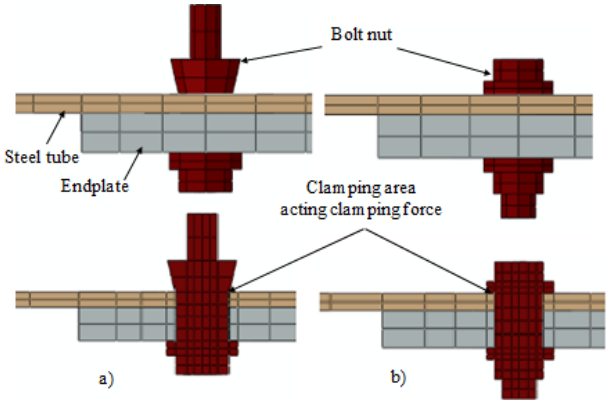

Figure 4: *FE modelling of blind-bolted endplate connections with: a) simplified Hollo-bolt; b) Ajax ONESIDE bolt or normal bolt*

Table 1: *Dimension details of simplified Lindapter Hollo-bolt M16 and M20 of grade 8.8 (unit: mm)*

Product Code	Bolt size	Bolt Diameter D_1	Clamping thickness range (W)	Sleeve		Collar		Clamping thickness (t_2)	Solid Cone thickness (t_3)	Cone angle /slope
				Length (L)	Outer diameter (D_2)	Height (t_1)	Outer diameter (D_3)			
HB16-1	M16	16	12-29	41.5	27.75	8	38	a	L- t_2	15
HB16-2	M16		29-50	63				a	L- t_2	
HB16-3	M16		50-71	84				a	L- t_2	
HB20-1	M20	20	12-34	50	32.75	10	51	a	L- t_2	15
HB20-2	M20		34-60	76				a	L- t_2	
HB20-3	M20		60-68	102				a	L- t_2	

Note: a= the sum of the steel tube thickness and endplate thickness

another. The surfaces, which come into contact (as shown in Figure 5) and are assigned as surface to surface contact, are inner surface of the steel tube to outer surface of concrete core (Contact A), endplate to outer surface of steel tube (Contact B), bolt head to endplate (Contact C), bolt shank to bolt holes (Contact D), bolt nut to inner surface of steel tube and concrete core (Contact E).

In the surface-to-surface contact, the master surface and slave surface need to be carefully defined for contact formulation. It is also required to define the contact sliding formulation option and the contact interaction properties. The contact sliding formulation uses the finite sliding. To define the contact interaction properties, two properties are required; one is normal interaction and another one is tangential interaction. The normal interaction between the surfaces is defined as a "hard contact". The tangential behaviour of surface to surface contact is defined using the Coulomb friction model where the tangential motion will be zero until the surface traction reaches a critical shear stress value. This critical shear stress can be calculated from the function of normal contact pressure and friction coefficient. This function is defined as $\tau=\mu P$, where τ is the critical shear stress, P is the normal contact pressure and μ is the friction coefficient of the contacting surfaces and assigned the value of 0.25 for all contacting surfaces of joint components [7-8].

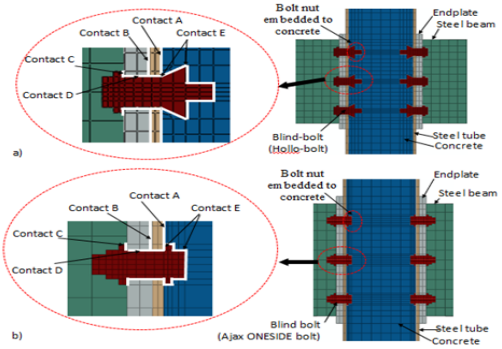

Figure 5: *Contact details for steel beam-CFST column joints with: a) blind-bolted (Hollo-bolt) endplate connection, b) Ajax ONESIDE or normal bolted endplate connection*

2.4 MATERIAL MODELLING

The material properties for various components of beam-CFST column joints are determined from the material test data in the form of the engineering stress (σ_{eng}) and strain (ε_{eng}). But to simulate the connection behaviour more realistically in the FE analysis, the material property has to be defined by the use of the true stress and the true plastic strain relationship. The values of the true stress (σ_{true}) and the true plastic strain ($\varepsilon_{pl,true}$) are determined from the engineering stress and logarithmic strain relationship using the equations: $\sigma_{true} = \sigma_{eng}\left(1+\varepsilon_{eng}\right)$; $\varepsilon_{pl,true} = ln\left(1+\varepsilon_{eng}\right) - \frac{\sigma_{true}}{E}$. The stress-strain relationship of concrete, structural steel sections and structural bolts can be calculated from the material models proposed in the literature.

2.4.1 Concrete

The damage plastic model available in ABAQUS is often adopted for concrete in FE analysis. Eurocode model [9], Mander et al.'s model [10], Han et al.'s model [11], Tao et al.'s model [12] are available to simulate the concrete behaviour. Tao et al. [12] proposed a full-range stress-strain curve to represent the behaviour of confined concrete. The stress-strain relationship which is used in this paper is shown in Figure 6 and given as below:

$$\sigma = \begin{cases} \frac{A.X+B.X^2}{1+(A-2)X+(B+1)X^2} f_c' & 0 < \varepsilon \le \varepsilon_{co} \\ f_c' & \varepsilon_{co} < \varepsilon < \varepsilon_{cc} \\ f_r + (f_c' - f_r)\, exp\left[-\left(\frac{\varepsilon-\varepsilon_{cc}}{\alpha}\right)^{\beta}\right] & \varepsilon \ge \varepsilon_{cc} \end{cases} \quad (1)$$

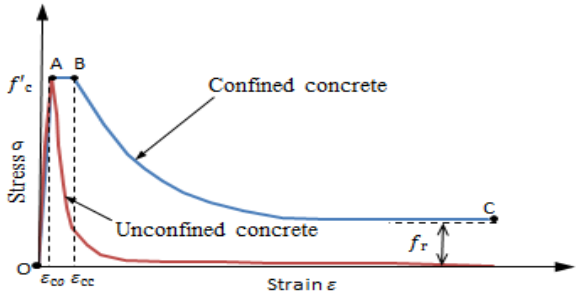

Figure 6: *Stress–strain model of confined concrete proposed by Tao et al. [12]*

The damage plastic model allows a multi-linear uniaxial compression stress-strain curve and tensile behaviour to be input. Other parameters such as dilation angle (ψ), eccentricity (e), ratio of the biaxial compression strength to uniaxial compression strength of concrete (f_{b0}/f_{c0}), the ratio of the second stress invariant on the tensile meridian to that on the compressive meridian (K), and viscosity parameter, are provided in ABAQUS. The modulus of elasticity of concrete (E_c) is equal to $4730\sqrt{f_c'}$ recommended by ACI Committee 318. The poison's ratio (v_c) is equal to 0.2. The default values of $\psi, e, K_c, f_{b0}/f_{c0}$ used are 30°, 0.1, 1.16 and 2/3 respectively.

2.4.2 Structural Steel

There are many material models available to describe the constitutive behaviour of steel [13-14]. Tao et al. [13] developed a stress-strain curve for structural steel and considered three parts including 1) elastic; 2) yielding; 3) hardening. This material model is used to derive the stress-strain relationship of the steel tube, steel beam, endplate, and binding bar.

2.4.3 Blind bolts

The mechanical behaviour of structural bolt materials is normally different from the structural steel section materials. Ductility of structural bolt materials is normally much lower than that of structural steel section materials. The mechanical behaviour of these materials for both tension and compression are assumed to be

similar although resisting capacity under compression is lower than that in tension. In general, bilinear and tri-linear stress-strain curves can be used to describe the structural bolt materials. Hanus et al. [15] reported a multi-linear stress-strain curve proposed by Riaux (1980) which considered three parameters, such as yield stress, ultimate stress and fracture stress. In this paper, the full-range stress-strain curve is used to define the behaviour of structural bolts.

2.5 NON-LINEAR FE ANALYSIS

Nonlinear behaviour of the steel beam to CFST column connections can be incorporated in the FE model by considering the three types of nonlinearities: material nonlinearity, geometric nonlinearity and boundary nonlinearity. Material nonlinearity of each component of the joint is assigned by applying the nonlinear stress-strain relationship. The geometric and boundary nonlinearities are assigned in the FE model using NLGEOM and CONTACT PAIR commands respectively in ABAQUS. Boundary nonlinearity is associated with a change in the boundary conditions (contact/gaps) during the analysis.

In the FE modelling, the loads are applied to reflect the actual loading condition. In a test, three types of loads are generally applied. These loads are bolt tightening force i.e. pretension force, column axial load and beam load. These loads are applied in three steps in FE modelling. In the first step, pretension force is applied through the "bolt load" option available in ABAQUS. The axial load on the column and beam load are applied in the second step and third step respectively by using either the load control method or displacement control method. The loading process is performed by adopting a general static analysis in which Newton-Raphson method is considered. This method is a powerful technique for solving equations numerically and to obtain the solutions for nonlinear problems. The nonlinear analysis is done by applying the load in increments and many iterations are required to solve the equations at a given load increment.

3 FE MODEL VALIDATION

Finite element analysis can be a reliable method to investigate the behaviour of steel beam-CFST column joints, provided its accuracy is verified by test results. The FE modelling details for blind-bolted endplate connections are illustrated in the previous sections. Numerous experimental works on blind-bolted (Hollo-bolt) endplate connections are available in the open literature. Reasonable agreement is obtained between the test results and predictions using the current FE model. Due to the page limitation, only a few test specimens are used to demonstrate the validation of the FE model. The details are given in the following sub-sections.

3.1 BLIND-BOLTED (AJAX) END PLATE CONNECTION TO SHS COLUMN IN TENSION

FE model for blind-bolted T-stub connections is developed and validated by the tests conducted by Lee et al. [16], in which the behaviour of blind bolted T-stub connections for square hollow section (SHS) columns was investigated. In this paper, two specimens (S1 & S2) conducted by Lee et al. [16] are considered. The main difference between these two test specimens is in bolt sleeves. In specimen S1, bolt sleeves are not utilised, but bolt sleeves are utilised in specimen S2 to cover the bolt hole. Both specimens (S1 & S2) comprised of a hollow SHS column with a cross-section of 150×150×6 mm of Grade 350 MPa. The blind bolt (Ajax ONESIDE bolt) of Grade 8.8 M16 (yield strength=640 MPa, minimum tensile strength=800 MPa) and endplate 270×150×10 mm of Grade 300 MPa are utilised in these tests. The Ajax ONESIDE bolts are modelled like normal bolts because the geometry of the Ajax ONESIDE bolt after tightening is almost similar to that of normal bolts. Material and geometric nonlinearities are taken into account in the FE model as described in section 2. Displacement control method is considered for loading applied via the stem of the T-stub with a thickness of 20 mm of Grade 300 MPa. C3D8I elements are used for all components in the joint. The FE model results and the test results presented by Lee et al. [16] are compared in Figures 7 and 8. Figure 7 shows the failure mode of the tube, i.e. punching failure of the bolt holes. Comparison between the observed failure mode of the tube and the FE model result shows good agreement. Figure 8(a) shows a comparison between experimental and FE model results of specimen S1 in which the blind bolts did not have sleeves. The gap between the bolt shank and bolt hole was 8 mm (16 mm diameter bolt with a 24 mm diameter bolt hole as mentioned in Lee et al. [16]). Figure 8 (b) shows a comparison between experimental and FE model results of specimen S2. The presence of the sleeves in specimen S2 which fill the gap between the oversized hole and bolt shank (reducing the gap from a total 8 mm to 0.5 mm) reduced the bending of the bolts and hence increased the ultimate strength compared to the ultimate strength of the specimen S1 as shown in Figure 8(a).

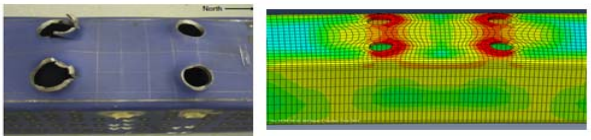

Figure 7: *Failure mode and stress contour of the panel zone of the tube (Specimen S2)*

3.2 BLIND-BOLTED END PLATE CONNECTION TO CFST COLUMN IN TENSION

FE modelling of a CFST column to steel beam joint with blind bolted (Hollo-bolt) endplate connection is quite different from that of the unfilled-steel tubular column to steel beam joint with blind bolts. Six tests on blind bolted (Hollo-bolt) endplate connections were conducted under tension and the test results were reported by Li et al. [17]. The configuration of one of the steel beam-CFST column joints is shown in Figure 9 and the mechanical properties of the joint components are given in Table 2. The FE model is developed as shown in

Figure 10(a) and validated with the experimental test data. In the FE modelling, only half of the specimen was considered in order to reduce the size of the model and, consequently, the computational cost, by applying the appropriate boundary conditions. To demonstrate the effect of using different bolts, the FE model of the joint with Ajax ONESIDE or normal bolts is also developed as shown in Figure 10(b). Loads are applied in two steps: Bolt tightening force i.e. pretension force (125 kN) is applied in the first stage through the "bolt load" option available in ABAQUS, and in the second stage, tensile loading acting on the beam longitudinal direction is applied through the displacement control. C3D8I elements are adopted for all components used in the joint.

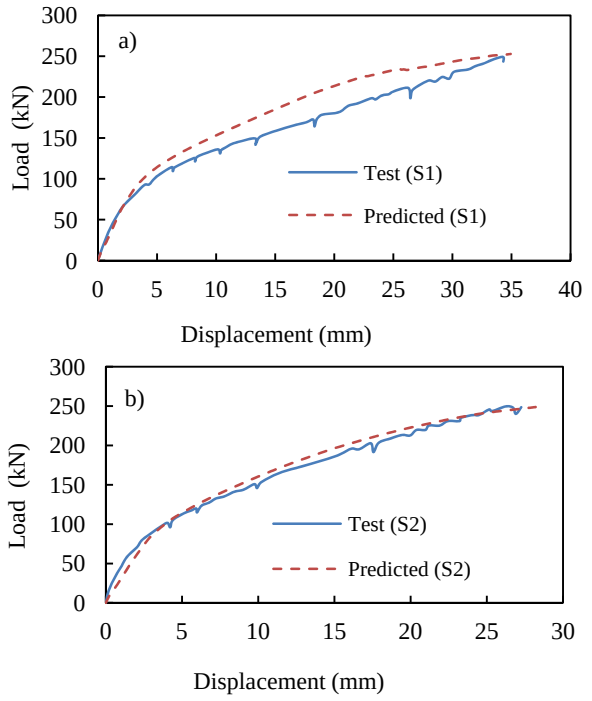

Figure 8: *FE model validation with experiment conducted by Lee et al. 2010: a) Specimen S1; b) Specimen S2*

The FE model result of blind-bolted (Hollo-bolt) endplate connection is compared with the test result as shown in Figure 11. Meanwhile, the Ajax ONESIDE bolted (i.e. normal bolt, Grade 8.8 M20) endplate connection is also modelled and compared with the blind-bolted (Hollo-bolt, Grade 8.8 M20) endplate connections model. The FE model result of the blind-bolted (Hollo-bolt) endplate connection shows a good agreement with the test result. It is also observed from FE results that the load-displacement behaviour of the blind-bolted (Hollo-bolt) endplate connection differs from that of the Ajax ONESIDE bolt or normal bolted endplate connection. The main differences are in the initial stiffness and ultimate load capacity. The initial stiffness of the blind-bolted (Hollo-bolt) endplate connection is found to be higher than that of the Ajax ONESIDE or normal bolted endplate connection. Because the Hollo-bolts especially their nuts with a cone shape are embedded in the concrete core of the CFST column and form a secure clamping against pull out. For other bolts, nuts are in hexagonal shapes (modelled as a round shape) which interact less with concrete and have no securing clamping resistance against pull out. As a result the stiffness and ultimate capacity found from the FE prediction of the Ajax ONESIDE bolt or normal bolted endplate connection is lower than the values of the corresponding joints with Hollo-bolts. This emphasises the fact that the geometry and contact properties should be modelled properly for Hollo-bolted endplate connections.

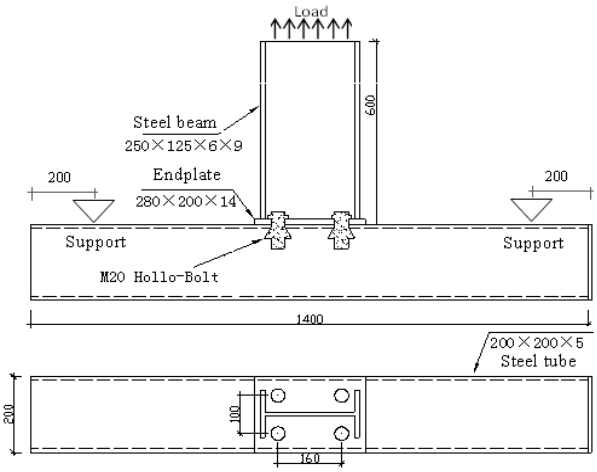

Figure 9: *Configuration details of the blind-bolted endplate connection for a steel beam-CFST column joint*

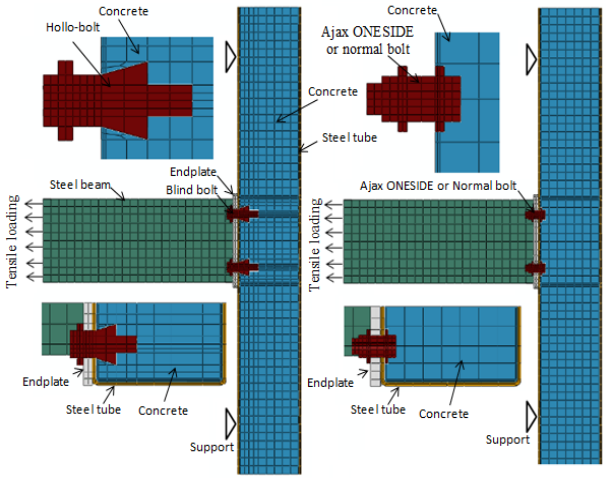

Figure 10: *FE model of steel beam-CFST column joints in tension with: a) blind-bolted (Hollo-bolt) connection, b) Ajax ONESIDE or normal bolted connection*

Table 2: *Mechanical properties of joint components (All units are in MPa)*

Items	Yield stress	Ultimate stress	Elastic modulus
Steel tube	308	439.2	216000
Flange of beam	247.4	405.4	217850
Web of beam	267.1	410.5	201075
Endplate	270.8	438.8	209117
M20 Hollo-bolt	747.5	884.7	218500

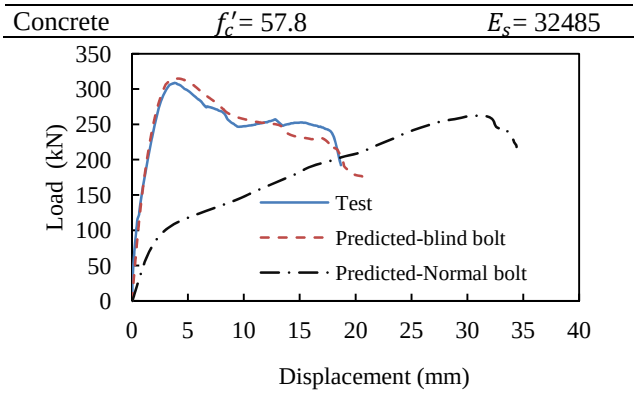

Figure 11: *Comparison between FE model and test of a blind bolted endplate connection under tension*

3.3 BLIND-BOLTED ENDPLATE CONNECTION TO CFST COLUMN IN BENDING

A FE model of blind-bolted (Hollo-bolt) endplate connection to CFST column in bending was developed for the specimens conducted by Wang et al. [18]. In the FE modelling, only half of the joint specimen was modelled as shown in Figure 12. All components of the joint are modelled using C3D8I elements except the steel beam which is modelled using shell elements (S4R). The yield strengths of the steel tube, steel beam flanges and web, endplates and bolts were 301.7 MPa, 262.3 MPa, 272.8 MPa, 268.5 MPa, and 752 MPa, respectively. The concrete compressive cube strength (f_{cu}) was 32 MPa. Other material properties and specimen details including dimensions are available in Wang et al. [18]. In the FE modelling, three types of loads are considered and applied in three steps. In the first step, bolt tightening force i.e. pretension force (125 kN) is applied through the bolt loading option available in ABAQUS. Then the column axial load (60% of the CFST column capacity, 1777 kN) is applied in the second step through the load control method, and finally the bending load acting at the beam's tip is applied in the final step through the load control method.

The results obtained from the FE model of blind-bolted (Hollo-bolt, Grade 8.8 M16) endplate connection subjected to bending loading are compared with the test results presented by Wang et al. [18]. The FE results show good agreement with the test results as shown in Figures 13 and 14 for specimens CJM1 and CJM2, respectively. The predicted initial stiffness shows a good correlation with the test results, and the ultimate capacity from the FE prediction is only 2-5% higher than the measured strengths for specimen CJM1 & CJM2.

4 PARAMETRIC ANALYSIS

The above verified FE modelling technique is used to conduct a parametric analysis. Two parameters are considered: one is the blind bolt type (Hollo-bolt and Ajax ONESIDE bolt); another is the existence of the binding bars. The binding bars are used as stiffeners in the steel tube to reduce the separation of the steel tube from the concrete core of the CFST column. In conducting the parametric analysis, the specimen CJM1 presented by Wang et al. [18] is used as an example. The binding bars are placed either above or below the top row of the bolts or at both locations.

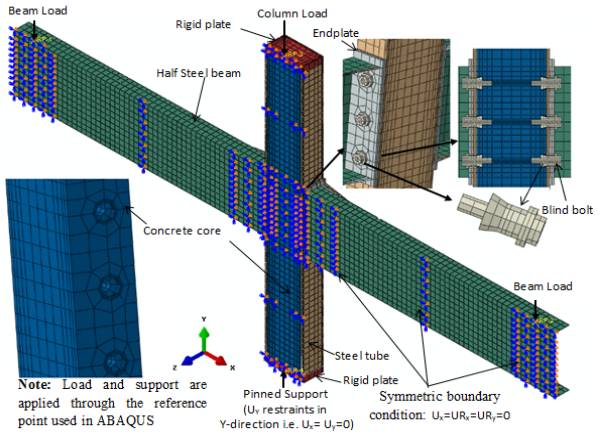

Figure 12: *FE model details of blind bolted (Hollo-bolt) endplate connection to CFST column in bending*

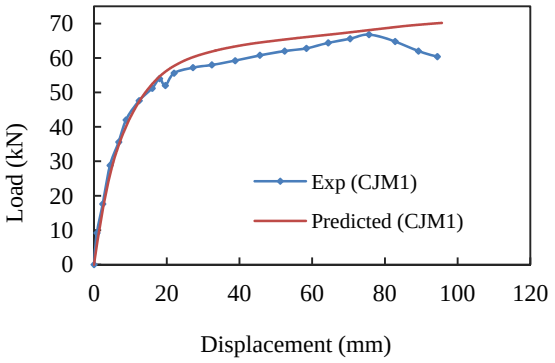

Figure 13: *Comparison between FE prediction and test (specimen CJM1) conducted by Wang et al. [18]*

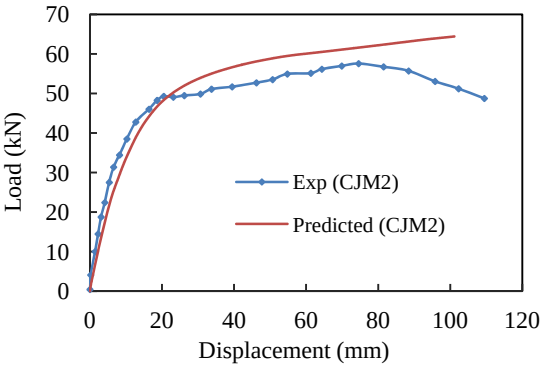

Figure 14: *Comparison between FE prediction and test (specimen CJM2) conducted by Wang et al. [18]*

4.1 EFFECT OF DIFFERENT TYPES OF BLIND BOLTS

The behaviour of blind-bolted endplate connections has been investigated by several researchers, but no comparative studies have been reported on the influence of different types of blind bolts. FE models are developed in this paper to investigate the difference

when Hollo-bolts or Ajax ONESIDE bolts are used to connect the steel beam to CFST column.
The FE model result of the Ajax ONESIDE bolted (Grade 8.8 M16) endplate connection is compared with the FE prediction of the Hollo-bolted (Grade 8.8 M16) endplate connection in Figure 15, where the load and deformation are those at the tip of the beam. From the comparison, it is seen that the ultimate load capacity of the Hollo-bolted endplate connection is higher than that of the Ajax ONESIDE bolted endplate connection. At a displacement of 100 mm, the ultimate strengths are 71.5 kN and 64.2 kN for the joints with Hollo-bolts and Ajax ONESIDE bolts, respectively. Due to the good mechanical bonding between the concrete and bolt nut of Hollo-bolts, the corresponding joints have higher strength. But the influence of the bolt type is not as significant as shown in Figure 11, in which the beam is in tension and bolts are subjected to pull-out force.

Figure 16 shows the horizontal deformation of the steel tube at the top row of the bolts for connections using different bolts. More obvious separation of the steel tube from the concrete core is observed for the Ajax ONESIDE bolted endplate connections compared with the Hollo-bolted endplate connections. This can be more clearly seen from the failure modes shown in Figure 17. It can be concluded that the steel tube outward deformation can be reduced by utilising Hollo-bolts in blind-bolted endplate connections.

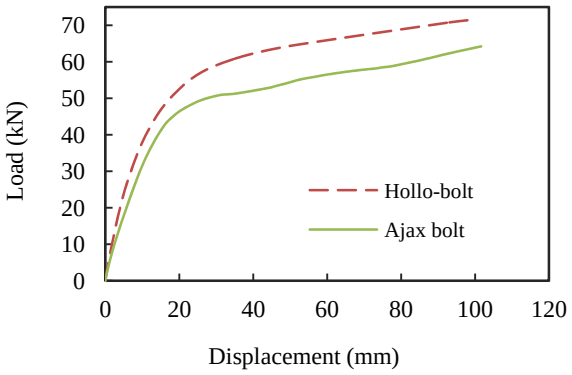

Figure 15: *The influence of bolt type on the load-deformation curve*

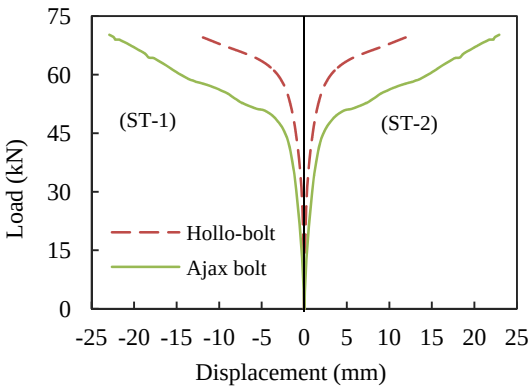

Figure 16: *Outward deformation of the steel tube at the top row of the bolts for connections with different types of bolts*

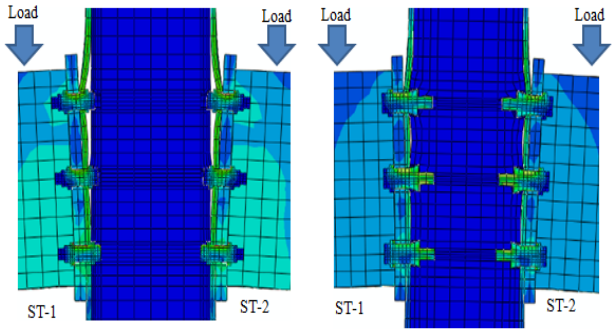

Figure 17: *Failure modes of endplate connections (Specimen CJM1): a) with Ajax bolts; b) with Hollo-bolts*

4.2 EFFECT OF BINDING BARS

The separation of the steel tube from the concrete in the CFST column is one of the most common phenomena observed in endplate connections when the tensile load or bending moment from the beam is transferred to the steel tube of the CFST column [8]. To reduce this steel tube separation, binding bars are proposed to be used as stiffeners on the steel tube. Binding bars can be welded on the steel tube to connect the opposite faces of the steel tube, thus increasing the integrity of the panel zone. Four case studies are conducted to find out the effective number of binding bars and their locations.

Figure 18 shows the load-displacement curves of four joints with different binding bar's arrangements such as "0-binding bars" (without binding-bars), "2-binding bars ATB" (2 binding bars are used above the top row of the bolts (ATB)), "2-binding bars BTB" (2 binding bars are used below the top row of the bolts (BTB)), "4-binding bars" (4 binding bars are used at locations above and below the top row of the bolts (ATB)). The top binding bars and bottom binding bars are placed at distances of 45 mm and 52 mm away from the centre of the top bolts, respectively. At a displacement of 100 mm, a capacity of 90.90 kN is obtained for the Hollo-bolted endplate joint with 4 binding bars (shown as "4-binding bars" in Figure 18), whilst a capacity of 71.54 kN is obtained for the reference joint without any binding bars (shown as "0-binding bars" in Figure 18). When two binding bars are used either at a location above or below the top bolts, the load capacity is also increased compared with that of the reference joint. It appears therefore that the two binding bars can be arranged either above or below the top bolts in the case of "2-binding bars ATB" as compared with the case of "2-binding bars BTB" as shown in Figure 18.

Figure 19 shows the steel tube outward deformation of blind-bolted endplate connections with different number of binding bars. The steel tube outward deformation is significantly influenced by the number of binding bars. At a beam deflection of 100 mm, the steel tube buckling i.e. outward deformation near the top bolts is significant (12.6 mm) for the blind-bolted endplate connection without binding bars. On the other hand, the steel tube deformation is less significant for the blind-bolted endplate connections with binding bars. With increasing number of binding bars, the load capacity of the joint

increases, but the steel tube outward deformation decreases.

Figure 20 shows the steel tube deformation at a specific load (70 kN) for different joints. From the comparison, it can be concluded that the steel tube outward deformation is greatly reduced and the integrity of the connection is enhanced by providing binding bars.

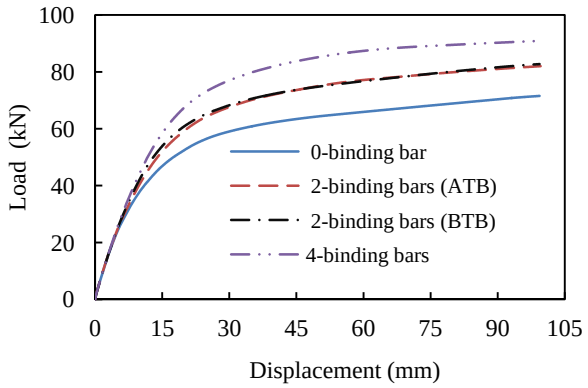

Figure 18: *Effect of binding bars on the load-displacement behaviour of steel beam–CFST column joints*

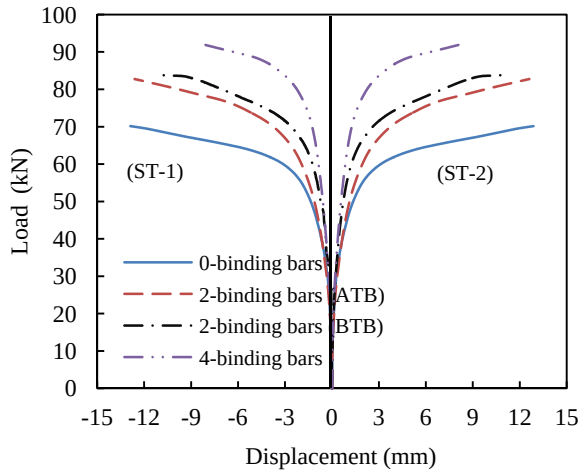

Figure 19: *Outward deformation of the steel tube near the top bolts for joints with different numbers of binding bars*

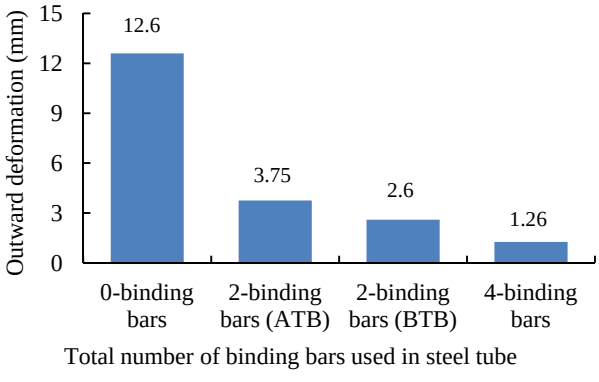

Figure 20: *Steel tube outward deformation at a certain load (70 kN) for joints with different numbers of binding bars*

5 CONCLUSIONS

In this paper, a FE model has been developed for steel-beam-CFST column joints. The FE modelling generally depends on the proper consideration of element types, geometry modelling of joint components (especially for Hollo-bolts), contact interaction, and material modelling. The following conclusions can be drawn based on the studies of this paper:

a) From the element sensitivity analysis, it can be concluded that C3D8R elements are more sensitive to meshing in modelling steel beam-SHS column joints, whilst C3D8I, C3D20, C3D20R elements give more accurate results compared with C3D8R elements. But the computation time is much higher when elements C3D20 or C3D20R are used rather than C3D8I elements. To optimise the computational time and to get accurate results, C3D8I elements are recommended for use in modelling joint components such as the steel tube, steel beam, endplate, bolt and concrete core.

b) A simplified model was proposed for Hollo-bolts. The modelling of Ajax ONESIDE bolts was also considered in this study. FE models of joints with Hollo-bolts and Ajax ONESIDE bolts have been developed and validated with experimental test data. The FE model results show good agreement with the test results.

c) The influence of different types of blind bolts (Hollo-bolt and Ajax ONESIDE bolt) on the joint performance was investigated. The load capacity of the joint with Hollo-bolts is higher than that of the joint with Ajax ONESIDE bolts. The steel tube separation from the concrete core of the CFST column is more significant when the Ajax ONESIDE bolts are used.

d) Binding bars can be used to minimise the steel tube separation or outward deformation. With increasing number of binding bars, the load capacity of the joint increases, but the steel tube outward deformation decreases.

ACKNOWLEDGEMENT

This work is supported by the Australian Research Council (ARC) under its Discovery Project scheme (DP120100971). The financial support is gratefully acknowledged.

REFERENCES

[1] Tao Z., Uy B., Han L. H., Wang Z. B.: Analysis and design of concrete-filled stiffened thin-walled steel tubular columns under axial compression. *Thin-Walled Structures,* 47(12): 1544-1556, 2009.

[2] Uy B., Tao Z., Han L. H.: Behaviour of short and slender concrete-filled stainless steel tubular

columns. *Journal of Constructional Steel Research,* 67(3): 360-378, 2011.

[3] Mirza O., Uy B.: Behaviour of composite beam-column flush end plate connections subjected to low-probability, high-consequence loading. *Engineering Structures*, 33(2): 647-662, 2011.

[4] Kurobane Y., Packer J., Wardenier J., Yeomans N.: Design guide for structural hollow section column connections. Köln, Germany: TÜV-Verlag, 2004.

[5] Bursi O. S., Jaspart J. P.: Basic issues in the finite element simulation of extended end plate connections. *Computers and Structures*, 69: 361-382, 1998.

[6] Sarraj M.: The behaviour of steel fin plate connections in fire. PhD Thesis, Department of Civil and Structural Engineering, The University of Sheffield, 2007.

[7] Huang C. S., Hu H.T., Chen Z.L.: Finite element analysis of CFT columns subjected to an axial compressive force and bending moment in combination. *Journal of Constructional Steel Research*, 61(12): 1692-1712, 2005.

[8] Hassan M. K., Tao Z., Uy B.: Effect of binding bars on the integrity of end plate connections to concrete-filled stainless steel tubular columns. *Proceedings of the 10th Pacific Structural Steel Conference on Singapore,* 297-302, 2013.

[9] Eurocode 2. 2005. Design of concrete structures, Part 1-1, General rules and rules of building. BS EN 1992-1-1: 2002. British Standards Institution, London; 2005.

[10] Mander J. B., Priestley M. J. N., Park, R.: Seismic design of bridge piers. Research Report No. 84-2, University of Canterbury, New Zealand, 1984.

[11] Han L. H., Wang W. D., Zhao X. L.: Behaviour of steel beam to concrete-filled SHS column frames: Finite element model and verifications. *Engineering Structures*, 30(6): 1647-1658, 2008.

[12] Tao Z., Wang Z. B., Yu Q.: Finite element modelling of concrete-filled steel stub columns under axial compression. *Journal of Constructional Steel Research*, 89: 121–131, 2013.

[13] Tao Z., Wang X. Q., Uy B.: Stress-strain curves of structural steel and reinforcing steel after exposure to elevated temperatures. *Journal of Materials in Civil Engineering*, 25(9):1306–1316, 2013.

[14] Eurocode 3. Design of steel structures, Part 1-1, General structural rules. prEN 1993-1-1: 2001.

[15] Hanus F., Zilli G., Franssen J. M.: Behaviour of Grade 8.8 bolts under natural fire conditions—Tests and model. *Journal of Constructional Steel Research*, 67(8): 1292-1298, 2011.

[16] Lee J., Goldsworthy H. M., Gad E.F.: Blind bolted T-stub connections to unfilled hollow section columns in low rise structures. *Journal of Constructional Steel Research,* 66(8-9): 981-992, 2010.

[17] Li D. S., Tao Z., Wang Z. B.: Experimental investigation of blind-bolted joints to concrete filled steel columns. *Journal of Central South University* [submitted for publication].

[18] Wang J. F., Han L. H., Uy B.: Behaviour of flush end plate joints to concrete-filled steel tubular columns. *Journal of Constructional Steel Research*, 65: 925-939, 2009.